Names of the Authors

1. Fatima Akter (Corresponding author)

Email: fatima_a@storm.dpri.kyoto-u.ac.jp

Present address: Disaster Prevention Research Institute,

Kyoto University, Gokasho, Uji, Kyoto-611-0011, Japan

Phone : +810774-24-4162

2. Hirohiko Ishikawa

Email: ishikawa@storm.dpri.kyoto-u.ac.jp

Professor, Disaster Prevention Research Institute,

Kyoto University, Gokasho, Uji, Kyoto-611-0011, Japan

Title

Synoptic and Environment conditions of the 22 March 2013 Tornado event in Brahmanbaria - the central east part of Bangladesh

1 Introduction

Bangladesh is vulnerable to various natural hazards. Severe Local Convective Storms (hereinafter referred to as SLCS) is one of the most devastating phenomena in the pre-monsoon months (March-May) in Bangladesh and adjoining North Eastern India. The SLCS accompany gusty wind, heavy downpours and hails after a long dry season, and often spawn tornadoes. SLCS cause huge damages to our lives and properties in a very short period. These storms are locally termed as Nor'wester (*Kalbaishakhi*- in Bengali) since the system migrates from north-west to south-east. Every year the SLCS of Bangladesh cause the highest death toll in the World. Annual death toll accounts for 179 deaths per year caused by only from tornadoes in Bangladesh from the period of 1967-96 (Ono 2001).

On 22 March, 2013 a devastating tornado (approximately 15mins) hit the villages in Sadar upazila (regional subdivision - the second lowest administrative unit) (24˚N latitude and 91˚E longitude) of Brahmanbaria district in central east part of Bangladesh (Fig.1a). It was initiated in the afternoon 1055 UTC (the Bangladesh Local Time is UTC + 6 hour) and was extinguished at 1110 UTC according to the eye witness. Thirty six persons were killed and three hundred eighty eight persons were injured by this event[1]. The tornado left a trail of destruction stretching as long as 12-15 km length passing over 22 villages and the width was approximately 100 to 150 m. A GPS tracking of the tornado path was conducted by SAARC Meteorological Research Center (SMRC) after the event occurrence (Fig. 1b). The wind speed was approx. 55 m/s. It was identified as F2 category in the Fujita scale[2].

In the pre-monsoon season, surface warm moist southerly wind blows from the Bay of Bengal towards Bangladesh whereas surface warm dry westerly blows from Indian territory. Strong horizontal moisture gradient is created between these two air masses of different origin.

[1] Situation Report, Disaster Management Bureau, Bangladesh
[2] BMD Newsletter, Vol.3, issue 3, May 2013

In the mid- and upper-troposphere there prevails strong cool dry north-westerly, which extends to westerly jet over the north-eastern part of Indian subcontinent. Intense insolation of this season heats the dry ground surface and a heat low develops in the lower troposphere over the Indian high land. In contrast the seasonal high is observed over the Bay of Bengal. Strong moisture gradient, temperature and pressure difference between dry and moist part, significant vertical wind shear and temperature inversion (2 km AGL) over moist side produce great potential instability and these weather conditions are favorable for frequent and intense convective activities in Bangladesh and North-east India (Weston 1972; Prasad 2006; Yamane and Hayashi 2006; 2010b). Previous studies also identified that central region of Bangladesh is the most preferred location of SLCS formation in Bangladesh (Peterson and Mehta 1981; Yamane et al. 2010a). From our 16 years study (1990-2005), total 2,324 SLCS events were identified in Bangladesh territory (Yamane et al. 2010a), which means around 145 SLCS events occurs per year on an average. Some other studies focused on the dynamic and thermodynamic aspects of the initiation of SLCS (Yamane et al. 2010b; Murata et al. 2011; Lohar and Pal 1995), or discussed on propagation and modes of organization of mesoscale convective systems (Dalal et al. 2012) and lower-, mid- and upper- tropospheric features for initiation of nor'westers (Ghosh et al. 2008). Mukhopadhyay et al. (2009) explained the formation mechanism of SLCS with interaction of large scale and meso-scale environment for specific cases over West Bengal. However, the physical process of storm genesis with trigger mechanisms of SLCS organization are not yet well studied in Bangladesh due to the scarcity of observation data in the study area.

In Bangladesh sparse surface weather stations, 3 active radar (not continuous) and only one upper air sounding at Dhaka (23.7N latitude and 90.3E longitude) limit the understanding of severe weather in Bangladesh. In the previous studies it was difficult to see the detailed environmental features for individual events. So, in this paper we attempt to confirm that reanalysis data successfully analyzes accurate environment conditions and trigger mechanism of convection initiation for SLCS occurrence in that particular area.

In order to minimize the SLCS disasters, proper prediction of convective event is important. Such a local scale phenomena as SLCS, however, is very difficult to predict numerically. Instead of predicting SLCS itself, numerical prediction of pre-storm environment is to be used to assess the possibility of SLCS outbreak. In this context Yamane et al. (2010b, 2012) suggest the use of thermodynamic parameters as guidance to the prediction of possible SLCSs, where atmospheric environment has high potential instability on SLCS days of Bangladesh. Though the horizontal resolution was coarse to identify locality of SLCS event in that study, a finer resolution reanalysis data is now available from some meteorological centers. The use of objective analysis will be quite promising in predicting the possibility of SLCS events.

The objective of the paper is to show the role of significant synoptic and environmental features to trigger the formation and intensification of SLCS associated with the tornado that occurred on 22 March, 2013. In this present study, we use 55 years Japanese reanalysis JRA-55 data (0.5625 degree horizontal resolutions, approximately 50 km) of Japan Meteorological Agency (JMA) to show the detail environment condition of the event area.

2 Radar, Satellite and Synoptic Observation on 22 March, 2013

Weather radar images of the tornado event were captured at Cox's Bazar (21.4˚N and 92˚E) station of BMD (Fig. 2 a-d). The image at 0800 UTC shows the emergence of the system (Fig. 2a). The next radar image at 0900 UTC, two hours before of the event, shows the system was much developed and moved southeastward (Fig. 2b). Then, several convective clouds were developing along a line running from the west-southwest to east-northeast over the Bengal plain. The weather radar image at 1100 UTC, corresponding to the tornado occurrence time, shows that the matured system migrated over the event location (Fig. 2c). The following radar image was 15 minutes after the event occurrence time that shows relatively weak system crossing the event site

(Fig. 2d). The radar was nearly 300 km away from the tornado occurrence site and was out of the Doppler mode observation area. So the detailed structure was not obtained.

IR imageries observed by MTSAT-2 of JMA are also used to see the convective activities. Fig. 3 (a - h) show 8 panels of half hourly snaps of IR imageries of MTSAT-2 of 22 March, 2013. The star sign denotes the place of the tornado occurrence. At 0801 UTC[3] (approximately 3 hours prior to the event) shows the emergence of small convective cloud (system no. 1) along 90.7˚E longitude and 24.3˚N latitude (Fig. 3a). This cloud appears to be the genesis of storm. The position of the convective cell is close to the event occurrence site. The cell is seen to have intensified and little extended toward east-southeast direction (Fig. 3b). Fig. 3b is overlaid with the 0900 UTC horizontal specific humidity distribution data from BMD and it shows an area of high specific humidity gradient from south-west to north-east. At 0901 UTC Fig. 3c shows a signature of new cell (system no. 2) at the south west of the previous cell. Pioneer cell (system no.1) is developed a strong convective cell and second one also becomes stronger and another new signature of convection (system no. 3) is observed at south west (Fig. 3d). At 1001 UTC (Fig. 3e) three convective cells (systems 1, 2 and 3) are found aligned in a south-west to north-east line and each of which looks like tailing anvil clouds in east-southeast direction. This anvil direction coincides with upper wind direction above 700 hPa. The convective cloud line follows the specific humidity gradient line (referring Fig. 3b again). The pioneer cell (system no.1) becomes an organized mature system (Fig. 3f).

A tornado occurred at 1055 UTC and continued up to 1110 UTC near 91˚E longitude and 24˚N latitude. At 1101 UTC systems 1 and 2 merged together (Fig 3g) and later the system 3 joined with the merged system passed through the event area (Fig. 3h). The upper layer cloud (anvil) flows to east-southeast but the system seems to move eastward. The systems are

[3] The time of MTSAT-2 data refer to the start of full disk scan. The observation time at study area is several minutes after the designated time.

maintained till it dissipated after crossing the event area. The half hourly satellite images suggest the existence of certain triggering mechanism along the heads of a series of convective cells.

3 Data and Methodology

SLCS studies are difficult in Bangladesh territory due to its localized characteristics and sparse observation network. Existing observations do not describe the event precisely. So we have to use analysis or reanalysis data. JRA-55 reanalysis data is the world’s first atmospheric global reanalysis which covers 55 years (1958-2012) with four-dimensional variational data assimilation system Ebita et al (2011)[4].

The base model is of TL319L60, so that the horizontal resolution is 0.5625 degree in longitudinal direction and approximately 0.5625 in latitudinal.It has 60 layers from surface to 0.1 hPa. The vertical resolution is finer near the surface for better representation of the planetary boundary layer processes. The data are provided 6 hourly. Many variables are provided among which we use geopotential heights, wind (zonal and meridional), temperature and specific humidity in this study. These data are supplied in model grid, and we also computed Mean Sea Level Pressure (MSLP) and pressure level data at standard levels (1000, 975, 950, 925, 900, 875, 850, 825, 800, 750, 700, 650, 600, 550, 500, 450, 400, 350, 300, 250, 200, 150, 100, 70, 50 hPa) for the use in stability parameter calculation.

Before using the reanalysis data, however, it is important to check whether the analysis is in harmony with observed data. We compared JRA-55 reanalysis data to radiosonde data archived at University of Wyoming[5]. Fig. 4 shows comparisons of Dhaka radiosonde profile and the profile of reanalysis data at nearest grid to the radiosonde site at the event day. The geopotential height is of course almost identical. The temperature profile is also in good

[4] http://jra.kishou.go.jp/JRA-55/index_en.html
[5] http://weather.uwyo.edu/cgi-bin/sounding?region=seasia&TYPE=TEXT%3ALIST&YEAR=2013&MONTH=03&FROM=2200&TO=2200&STNM=41923

agreement besides slight difference in boundary layer. Horizontal winds show some scatter in radiosonde data. The scatter in humidity is rather large in relative humidity. It is not appropriate to say which data is plausible since both data have difference representativeness. A radiosonde data is a snapshot along the path of ascending sensors whereas the reanalysis represent the average over, at least, grid distance. The statistical performance of JRA-55 reanalysis was also checked with radiosonde observation for March to May in 2013 and the correlation is shown in Table 1. Geopotential height again shows very good correlation in all levels. Temperature also has good correlation almost all levels except for lower levels. Horizontal wind components have good correlation in upper levels but the correlation decrease in lower levels. Though the correlation is relatively low in some variables in boundary layer, both reanalysis and radiosonde observation are consistent.

To examine environmental stability condition several stability indices are computed. Convective parameters are K Index (KI), Total Total (TT), Showalter Stability Index (SSI), Precipitable Water (PW) (Kg/m^2), Convective Available Potential Energy (CAPE) (J/kg), Convective Inhibition (CIN) (J/kg) and Lifted Index (LI). Kinematic parameters are Mean Shear (MS) (m/s), wind shear between the surface and 500 hPa wind (SHEAR0-500 hPa) and Storm Relative Environmental Helicity (SREH) (m^2/s^2). Combined parameters relating to the occurrence of tornado are also computed, which are Vorticity Generation Parameter (VGP) (m/s^2), Energy Helicity Index (EHI), and Bulk Richardson Number (BRN). The physical meaning of the indices is explained in previous works (e.g. Yamane et al. 2010b).

The analysis region is seen in Fig. 5a. Synoptic features are discussed over a domain covering 65˚E-100˚E and 5˚N-29˚N (Fig. 5a). The topography of this region contains high land to the western, northern and eastern sides. The Bay of Bengal is situated to the South and central part is the one of the largest deltas of the world, the Ganges-Brahmaputra-Meghna river delta, belongs to Bangladesh territory. In the west Chota Nagpur Plateau (900 m) of India, in the north there are the great Himalayan ranges, in the north east there are Garo Hills (450 m) and Khashi hills (1500 m), in the south east Chittagong Hill tracts (300 m) and high mountain ranges of Tripura and Mizoram (2000 m) . For the detail analysis the analysis domain is taken between 84˚-94˚ E longitude and 18˚-28˚ N latitude (Fig. 5b). The study area covers almost total land area of Bangladesh. The area belongs to deltaic plain where altitude is less than 10 m above sea level.

4 Results and Discussion

4.1 Synoptic analysis on 22 March, 2013

Atmospheric temperature and wind at the lowest model level, approximately 13 meters above model topography, and the Mean Sea Level Pressure (MSLP) over Indian subcontinent of 22 March 2013 are shown in Fig. 5 a-b. The time is 0600 UTC on March 22, 2013, that is the local noon time and is 5 hours prior to the tornado occurrence. High pressure existed over Bay of Bengal. South-westerly wind was conveyed warm moist air toward Bangladesh. Westerly wind was blown from Indian highland toward Bangladesh. Surface air temperature was high in dry Indian highland but was relatively low over Bangladesh territory. The surface temperature increased more than 10 degrees over Indian sub-continent from 0000 UTC (0600 BST) to 1200 UTC (1800 BST) but it was several degrees in Bangladesh. At 0600 UTC warm advection is analyzed near south coast toward the Bangladesh (fig. not shown). This warm moist advection can bring instability in lower atmosphere. In the morning easterly wind component was prominent near the surface Fig. 4b. Wind shear between surface and 500 hPa was 23.2 at 0000 UTC at event location (24°N and 91°E). At 0600 UTC it slightly increased to 23.3 m/sec wind shear between surface south-easterly wind (1.6 m/s) and the 500 hPa westerly wind (20.5 m/s). It further strengthened to 24.3 m/sec at 1200 UTC around event site. This wind shear was rather stronger than the statistical value in SLCS days as calculated by Yamane et al. (2010b) and was attributed to the upper layer tough as discussed in Yamane et al. (2012).

Surface specific humidity was higher over Bangladesh territory than west side of Indian territory. Specific humidity distribution (Fig. 6 a-c) exhibited higher values near the coast than the inland. That is consistent with the pre-monsoonal climatological studies by Romatschke et al. (2010) over this region. Surface specific humidity was range from 10 to 15 g/kg over Bangladesh. In contrast the surface specific humidity was lower, typically between 6 and10 g/kg over West Bengal of India. It reached to 15 g/kg at 0600 UTC around the east central region where the event occurred (Fig. 6b). It was evident that southern, eastern and central part became much moist than the north-western part of Bangladesh. Temperature increased slowly over the moist east side than Indian dry area (Fig. 5b). Looking at the vertical cross section at 24˚N latitude at 0600 UTC (Figure is not shown) east to west decrease of specific humidity is analyzed between 84°E and 94°E longitude and vertically from surface to about 600 hPa. The sharp change of specific humidity was specifically seen 88.5°E to 90.5°E (10-15g/kg) in the lower level up to about 900 hPa without any detectable inclination and west of this specific humidity was decreased 10g/kg to 6g/kg.

In relation to storm genesis in Great Plains in United States, a line of moisture discontinuity, which is termed as dryline, has been discussed. Dryline is a mesoscale narrow boundary separates moist maritime tropical air masses of Gulf of Mexico from continental tropical dry air masses of the deserts in the western Great Plains in the United States during the warm season (Fujita 1958; Miller 1959; Rhea 1966). During the spring and early summer, the convective storms are frequently initiated along the dryline. Thus, we examine specific humidity gradient in the present case. The strength of specific humidity gradient is computed by

$$|\nabla . q| = \sqrt{\left(\frac{\partial q}{\partial x}\right)^2 + \left(\frac{\partial q}{\partial y}\right)^2},$$

where q is specific humidity (g/kg). In this study we calculate specific humidity gradient g/kg over 100 km and identify maximum gradient line as dryline from the plot.

Dryline in our case was a line of strong moisture gradient between warm dry air mass of Indian highland and moist air mass of Bay of Bengal, which was aligned in south-west to north-east direction (Fig. 6 a-c). This line also coincides with the direction of cloud line (Fig. 3f). From 0600 UTC to 1200 UTC strong gradient region (6g/kg/100km) moved eastward and squeezed, and the sharpest moisture gradient (10 g/kg/100km) reached to 88.5˚E longitude at 1200 UTC (Fig. 6c). Though the analysis time (1200UTC) is one hour after the event, we can assume that the stronger gradient existed before the event occurrence.

Drylines are known as the zones of enhanced surface convergence in the Great Plains in United States. Strong surface horizontal convergence also coincided with dryline in our study area. Horizontal divergences are shown in Fig. 6 (d - f). We computed horizontal divergence,

$$\text{div } \mathbf{v} = \frac{\partial u}{\partial x} + \frac{\partial v}{\partial y}$$

Negative divergence is referred to as convergence. The greatest enhancement of low-level convergence was computed in the area where continental westerly flow encounters maritime south-westerly or southerly flow (Fig. 6d-f). This was also the place of the most intense moisture gradient (Fig. 6a-c).

4.2 Atmospheric Stability Conditions on 22 March, 2013

Atmospheric instability is a major determinant to estimate the possibility of the development of SLCS. Yamane and Hayashi (2006) have evaluated environmental conditions for the formation of severe local storms across the Indian subcontinent and mentioned high thermal instability and vertical wind shear occur in Bangladesh and the northeastern India during the pre-monsoon season.

The Skew-T Log-P is one of the most commonly used thermodynamic diagrams in weather analysis and forecasting using radiosonde soundings. The upper level sounding is available only at 0000 UTC at Dhaka. We referred to Wyoming Skew-T Log-P analysis of the upper wind sounding at 0000 UTC launched at Dhaka station. High instability is identified where CAPE was 1690 J/kg at 0000 UTC by Wyoming products (Fig. 7a). CAPE value is analyzed comparatively low value as 1409 J/kg by JRA-55 reanalysis data at the nearest grid to Dhaka station at 0000 UTC due to different calculation methods using different vertical levels (Fig. 7b). Though the plot suggests favorable atmospheric condition for convective initiation, Dhaka station is about 110 km apart from the event site. Skew-T Log-P diagram is also plotted with JRA-55 reanalysis data at the nearest grid point to event location (91˚E longitude and 24˚N latitude) on 22 March in Fig. 7(c - e) together with wind profile. Plot shows CAPE 1381 J/kg at 0000 UTC. Easterly was prominent at surface and wind veers upward. Strong westerly analyzed at 300 hPa (Fig. 7c). At 0600 UTC about 5 hours prior to the event occurrence analysis an inversion of temperature was evident from 950 hPa to 900 hPa (Fig. 7d). South-easterly to southerly wind became prominent and surface convergence influenced upward motion. Low level clock wise wind veer and strong westerly increased around 450 hPa is also analyzed. It also shows high CAPE (2207 J/kg) value. Instability decreased (CAPE 1282 J/kg) at 1200 UTC after the event occurrence (Fig. 7e).

In Table-2 the values of various stability parameters of present case are compared with statistical values. The last three columns presents the values computed from JRA-55 data at the nearest grid of event site for 0000, 0600 and 1200 UTC. In the first two column the statistical values of these parameters obtained for SLCS days (Yamane et al., 2010b) are shown. Mean and median value for all indices of SLCS days and non-SLCS days were determined with statistical significance with the confidence level of 99% (except for the TTI). Since their values are calculated with Dhaka rawinsonde data, the parameters are also computed from Dhaka radiosonde data and JRA-55 values near Dhaka at 0000 UTC, which also listed in the third and fourth column.

It should be noted that there are differences in vertical resolution of different data sources. Yamane et al. (2010b) used very raw rawinsonde observation of data, whereas JRA-55 data has

30 levels between surface and 200 hPa as seen in Fig. 4. Further, our Dhaka radiosonde values in the third column are computed from standard level data only. This difference may affects the values for CAPE, CIN, MS, SREH and the combined parameters slightly, but others are not since they are computed from standard level data.

The comparison between statistical mean values and current values in Table-2 suggested that the environment was unstable from the early morning. Most of the convective parameters were in unstable regimes and met the favorable condition for SLCS occurrence at 0000 UTC and 0600 UTC except for PW. At 0000 UTC CAPE value already exceeded the statistical mean value and the energy continued to accumulate till 0600 UTC. At 1200 UTC, one hour after the event occurrence, the CAPE value decreased in reanalysis data. It seems that a storm may have occurred in the reanalysis modeling. SSI value was favorable only at 0000 UTC. For kinematic parameters only SHEAR0-500 hPa shows increased shear as day advances and favorable for convection initiation comparing to mean values. Among the combined parameters EHI indicates greater than 1 at 0600 UTC, which suggests preferable condition for supercell storm occurrences. These favorable conditions have reduced at 1200 UTC, one hour after the event occurrence. Dhaka radiosonde and JRA -55 reanalysis data has difference in CAPE, CIN, SREH and combined parameters. JRA-55 analyzed little lower values than radiosonde data. Dhaka radiosonde data also showed very favorable condition at 0000 UTC though the event site is 110 km apart from the radiosonde site.

We also referred to the proposed threshold values for respective parameters of SLCS occurrence by various authors (Fuelbarg and Biggar 1994; Sadowski and Rieck 1977; Showalter 1953; Galway 1956; Huschke 1959; Moncrieff and Miller 1976; Colby 1984; Rasmussen and Blanchard 1998; Rasmussen and Wilhemson 1983; Davies and Johns 1993; Hart and Korotky 1991; Davis 1993 and Weisman and Klemp 1982) and confirmed that the current values suggest the environment truly unstable before the storm genesis.

In order to judge which stability indices are able to predict of the pre-storm environment and possibility of SLCS occurrence, we investigated spatial distribution of those parameters. Spatial distribution of CAPE (J/kg) is shown over Bangladesh (Fig. 8a –c). CAPE values were high in the moist part and it was significantly increased as the day advances. At 0000 UTC the environment exhibited little unstable (Fig. 8a). Later at 0600 UTC the environment revealed more favorable for storm genesis (Fig. 8b). CAPE reached more than 2000 (J/kg) over the moist area before the event. At 1200 UTC CAPE is decreased (Fig. 8c). One day temporal analysis of CAPE at the cross section of 24˚N latitude (Fig. 8d) revealed that the event area was most unstable before the convection initiation.

Spatial distribution of are also analyzed for SHEAR0-500 hPa, SREH, EHI, LI, PW, KI, SSI, TTI and CIN at 0600 UTC of the event day. Unstable value of SHER 0-500 >23, KI >30 and TTI > 70 cover large area around event site at 06 UTC, so that these parameters are difficult to identify the event location. EHI greater than one was identified in very narrow zone pointing the area of potential supercell storm occurrences (Fig. 9a). EHI is used to identify tornado potential by combining total CAPE with SRH in the lower 3 km. CAPE was identified relatively larger area in the moist side of dry line. The SRH which is calculated storm motion using mean wind speed from 0-6 km, is a measure of potential for cyclonic updraft produced through the tilting of horizontal vorticity by storm relative inflow. SRH (<100 m^2/s^2) in our study region did not reach the mean value (148 m^2/s^2) of Yanmane et al (2010b) 5 hours prior to the event but high SRH extended over the area of high CAPE. Thus due to the increased wind speed within a convectively unstable area EHI indicates much specified area for severe outbreak. Also LI analyzed less than -2 (Fig. 9c), and low value of SSI (Fig. 9e) analyzed around event occurrence regions better than other indices. At 0600 UTC environment was unstable but convection started two hour later at 0800 UTC from satellite images (Fig. 3a). The critical condition formed between the two analysis times. One day temporal analysis at the cross section of 24˚N latitude of EHI (Fig. 9b) and LI (Fig. 9d) also revealed that the event area was most unstable before the event occurring time. Negative LI exist over relatively wide area and continuing long time after the event occurrence and most negative value of SSI exist after the event at 1200 UTC at the north-west of the event site (Fig 9f). Among all of these indices EHI was a good prediction parameter of this event.

5 Discussions

Convection initiation along dryline depends on the synoptic and localized environment features of dryline where surface convergence is enhanced which promotes upward motion consequently air parcels force to their LFC in an unstable environment to initiate convection. The processes of localized deep convection and developments along the drylines were well investigated in the Great Plains (Bluestein and Parker, 1993; Ziegler and Rasmussen, 1998 and Hane et al., 1997).

Synoptic and environment features vary distinctly between dry side and moist side of the dryline. At the dry side temperature increased and thermal low developed in Indian highland as the day advances (Fig 5b). Diurnal difference of surface temperature was 10 degrees or more over Indian subcontinent from morning to evening. A deep, well mixed dry layer developed over the Indian highland from ground to about 680 hPa (Figure not includes). Westerly wind was analyzed in all levels and no wind veer in low level. Strong Jet prevailed over this region above 300 hPa. This deep upper westerly wind advected the deep mixed layer eastward side and it overlaid on surface moist south-westerly to southerly moist tongue.

At the day advances increase of surface temperature was smaller at moist side than dry side by few degrees. High MSLP was analyzed over Bay of Bengal and east side of dryline over Bangladesh territory. Surface winds turns towards the dryline and results enhanced surface convergence at the dryline, which can enhance lift and aid convective initiation. In the current case surface convergence induces upward motion near dryline. As day advances CAPE increased due to enhanced moisture incursions in the lower level from the Bay of Bengal at the east side of the dryline. But elevated mixed layer above the moist region acts like cap or lid over the moist part and protect release of instability. Dryline advances to the east and moisture gradient squeezed and localized convergence become stronger and lift moist air aloft. Eventually it forces air parcels to break the lid and reach their LFC to trigger deep convection. Presence of westerly wind strong wind shear maintained and enhanced the triggered convection and the westerly also conveys this system to eastward. The system intensified and became matured enough to spawn as tornado at Brahmanbaria. This mechanism is very similar to the Great Plains convection intimation along dryline as mentioned in Hane et al. 1997, Murphey et al. 2006 and Ziegler and Rasmussen 1998.

There can be another question how much the event day differ from other days. In order to check the uniqueness of the event day, we also analyzed two days the, 20th and 21th March, 2013) before the event day. Pre-monsoon weather condition was prevailing similar to event day. But, specific humidity (8 to 12 gm/kg at 0600 UTC) and SHEAR 0-500 hPa (12-14m/s) were relatively low over Bangladesh territory. As day advanced to 1200 UTC moisture intrusion is analyzed with a little increase of SHEAR 0-500 hPa in coastal area. For these two non-events days surface temperature increase from morning to evening was more rapid and the low level humidity was less than the event day. Convergence along dryline was not strong enough due to weak moisture inflow. Surface low moisture cannot create enough instability. Thus weak convergence along dryline could not be uplift air parcel to LFC on non-event days.

6 Summary

In the present study, we examined the synoptic and environmental conditions for the tornado case on 22 March, 2013 that is the severest in the recent past occurrences. SLCS studies are very difficult in the study region due to its localized characteristics and sparse observation network.

Convective parameters and synoptic conditions for the particular case are computed by 50 km resolution JRA-55 reanalysis data. This case study suggests that low level convergence along dryline lift the lower atmosphere up to the level of free convection in a significantly unstable environment, where the initial convection triggered. Environment condition is very favourable for severe convection and storm initiation comparing with statistical data. EHI is a good predictor to identify SLCS occurrence place. In the previous studies the data resolution was poor, so that the regional preference of storm genesis is not known. The use of good resolution reliable and homogenous data may produce better prediction of severe storm in this area. It is also suggested that better time resolution data is required for pointing the high risk regions.

Acknowledgements

The JRA-55 reanalysis data of JMA used in this study was provided by way of Meteorological Research consortium, a framework for research cooperation of JMA and Meteorological Society of Japan (MSJ). I am grateful to Prof. Hayashi T, Dr. Yamane Y and Dr. Murata F for providing me data and valuable suggestions and discussions. I am also thankful to Mr. Abdul Mannan for providing 3 hourly Synoptic data, Radar data from BMD and encouragement.

References

Bluestein HB, Parker SS (1993) Modes of isolated, severe convective storm formation along the dryline. Mon. Wea. Rev., 121, 1354–1372.

Colby FP (1984) Convective inhibition as a predictor of convection during AVE-SESAM-2. Mon. Wea. Rev. 112, 2239–2252.

Dalal S, Lohar D, Sarkar S, Sadhukhan I, Debnath GC (2012) Organizational modes of squall-type Mesoscale Convective Systems during premonsoon season over eastern India. Atmospheric research 106, 120-138

Davies JM, Johns RH (1993) Some wind and instability parameters associated with strong and violent tornadoes. 1. Wind shear and helicity, In: Curch C, Burges D, Doswell C, Davies-Jones R (ed) The Tornado: Its Structure, Dynamics, Prediction, and Hazard. Geophys. Monogr., No. 79: Ame. Geophys. Union, pp. 573–582.

Davies JM (1993) Hourly helicity, instability, and EHI in forecasting supercell tornadoes. Proc. 17th Conf. Severe Local Storms, St. Louis, MO: Amer.Meteor. Soc., pp. 107–111.

Ebita, A., S. Kobayashi, Y. Ota, M. Moriya, R. Kumabe, K. Onogi, Y. Harada, S. Yasui, K. Miyaoka, K. Takahashi, H. Kamahori, C. Kobayashi, H. Endo, M. Soma, Y. Oikawa, and T. Ishimizu, (2011), The Japanese 55-year Reanalysis "JRA-55": an interim report, SOLA, 7, 149-152.

Fuelbarg HE, Biggar DG (1994) The preconvective environment of summer thunderstorms over the Florida Panhandle.Weather Forecast. 9, 316–326.

Fujita TT (1958) Structure and movement of a dry front. Bull. Amer. Meteor. Soc., 39, 574–582.

Galway JG (1956) The lifted index as a predictor of latent instability. Bull. Amer. Meteor. Soc. 37, 528–529.

Ghosh A, Lohar D, Das J (2008) Initiation of Nor'wester in relation to mid-upper and low-level water vapor patterns on METEOSAT-5 images. Atmos. Res. 87 116.135.

Hane CE, Bluestein HB, Crawford TM, Baldwin ME, Rabin RM (1997) Severe Thunderstorm

Development in Relation to Along-Dryline Variability: A Case Study. Monthly Weather Review, vol.125.2, Pp 231-51

Hart JA, Korotky W (1991) The SHARP workstation v1.50 users guide. National Weather Service, NOAA: US. Dept. of Commerce, p. 30.

Huschke RE (1959) Glossary of Meteorology. Amer. Meteor. Soc. 638.

Lohar D, Pal B (1995) The effect of irrigation on pre-monsoon season precipitation over south West Bengal. India J. Climate, 8 (1995), pp. 2567–2570

Miller RC (1959) Tornado-producing synoptic patterns. Bull. Amer. Meteor. Soc., 40, 465–472.

Moncrieff M, Miller MJ (1976) The dynamics and simulation of tropical cumulonimbus and squall lines. Quart. J. Roy. Meteor. Soc. 102, 373–394.

Murata F, Terao T, Kiguchi M, Fukushima A, Takahashi K, Hayashi T, Arjumand H, Bhuiyan MSH, Choudhury SA (2011) Daytime Thermodynamic and Airflow Structures over Northeast Bangladesh during the Pre-Monsoon Season: A Case Study on 25 April 2010. Journal of the Meteorological Society of Japan, Vol. 89A, pp. 167-179

Mukhopadhyay P, Mahakur M, Singh HAK (2009) The interaction of large scale and mesoscale environment leading to formation of intense thunderstorms over Kolkata Part I: Doppler radar and satellite observations. J. Earth Syst. Sci. 118, No. 5, pp. 441–466

Murphey HV, Wakimoto RM, Flamant C, Kingsmill DE (2006) Dryline on 19 June 2002 during IHOP, Part I: Airborne Doppler and LEANDRE II Analyses of the Thin Line Structure and Convection Initiation. Mon. Wea. Rev., 134, 406-430.

Ono, Y., 1997: Climatology of Tornados in Bangladesh, 1990-1994. J. Met. , Vol. 22, No. 222, pp. 325-340.

Ono Y (2001) Design and adoption of household tornado shelters to mitigate the tornado hazard in Bangladesh. PhD Dissertation, Kent State University

Peterson RE, Mehta KC (1981) Climatology of Tornadoes of India and Bangladesh. Arch. Met. Geoph.

Biokl., Ser.B, Vol. 29

Prasad K (2006) Environmental and synoptic conditions associated with no'westers and tornadoes in Bangladesh – An appraisal based on numerical weather prediction (NWP) guidance products. 14th report of SAARC Meteorological Research Center, Dhaka, Bangladesh.

Rasmussen EN, Wilhemson RB (1983) Relationships between stormcharacteristics and 1200 GMT hodographs, low-level shear, and stability. Proc. 13th Conf. on Severe Local Storms, Tulsa, OK: Amer. Meteor. Soc., pp. J5–J8.

Rasmussen EN, Blanchard DO (1998) A baseline climatology of sounding derived supercell and tornado forecast parameters. Weather Forecast.13, 1148–1164.

Romatschke U, Medina S, Houze RA (2010) Regional, Seasonal, and Diurnal Variations of Extreme Convection in the South Asian Region, J. Climate, 23, 419-439.

Rhea JO (1966) A study of thunderstorm formation along dry lines. J. Appl. Meteor., 5, 58–63.

Sadowski AF, Rieck RE (1977) Technical Procedures Bulletin No. 207: Stability indices. National Weather Service, Silver Spring, MD, p. 8.

Showalter AK (1953) A stability index for thunderstorm forecasting. Bull. Amer. Meteor. Soc., 34, 250-252.

Yamane Y, Hayashi T (2006) Evaluation of environmental conditions for the formation of severe local storms across the Indian subcontinent. Geophys. Res. Lett. 33, L17806.

Yamane Y, Hayashi T, Dewan AM, Akter F (2010a) Severe local convective storms in Bangladesh: Part 1. Climatology. Atmospheric Research 95: 400-406.

Yamane Y, Hayashi T, Dewan AM, Akter F (2010b) Severe local convective storms in Bangladesh: Part 2. Environmental conditions. Atmospheric Research 95: 407-418.

Yamane Y, Hayashi T, Kiguchi M, Akter F, Dewan AM (2012) Synoptic situations of severe local convective storms during the pre-monsoon season in Bangladesh. International Journal of Climatology, 33: 725–734.

Weston KJ (1972) The dry-line of Northern India and its role in cumulonimbus convection. Quarterly Journal of the Royal Meteorological Society 98 (417): 519–531

Weisman ML, Klemp JB (1982) The Dependence of Numerically Simulated Convective Storms on Vertical Wind Shear and Buoyancy; Mon. Wea. Rev., Vol. 110, p. 504 - 520

Weisman ML, Klemp JB (1986) Characteristics of Isolated Convective Storms. In: Ray P (ed) Mesoscale Meteorology and Forecasting; American Meteorological Society, Boston, p. 331 – 358

Ziegler CL, Hane CE (1993) An observational study of the dryline. Mon. Wea. Rev.,121, 1134–1151.

Ziegler CL, Rasmussen EN (1998) The Initiation of Moist Convection at the Dryline: Forecasting Issues from a Case Study Perspective. Wea. Forecasting, 13, 1106-1131.

ABSTACT

This study evaluates the synoptic and environmental conditions of Brahmanbaria tornado event that caused 36 fatalities, 388 injuries and huge damages of properties on 22 March, 2013. Various factors for initiation of that terrific event are investigated through analysis JRA-55 reanalysis (50 km horizontal resolution) data and Multi-functional Transport Satellite (MTSAT) images by Japan Meteorological Agency (JMA). In addition, Radar images, radiosonday data and 3 hourly synoptic data of Bangladesh Meteorological Department (BMD) are used to verify the reanalysis data. The genesis of the tornadic storm is identifiable in the most unstable part of the study region. The satellite observations are found to useful to identify the location of convection occurrence region. The half hourly satellite images identify that the convection initiation started at the convergence area and the systems intensify and organize by the continuous moisture supply from the Bay of Bengal. Lower level convergence coupled with strong wind shear and humidity gradient lift moist air aloft to trigger deep convection and the severe storm occurred. Energy Helicity Index (EHI) seems a good predictor parameter for this specific case study.

Table -1 Data Validation Table

(a) 00 UTC

hPa / component	Geopotential heights	Zonal wind(m/s)	Meridional wind(m/s)	Temperature (K)	Specific humidity (g/kg)	Relative humidity (%)
1000	0.983	0.509	0.730	0.546	0.553	0.338
925	0.969	0.750	0.792	0.611	0.699	0.557
850	0.915	0.706	0.692	0.787	0.831	0.716
700	0.899	0.772	0.610	0.936	0.850	0.781
500	0.920	0.890	0.848	0.933	0.810	0.690
300	0.987	0.952	0.853	0.972	0.670	0.597
200	0.993	0.955	0.925	0.939	-	-

(b) 12 UTC

hPa / component	Geopotential heights	Zonal wind(m/s)	Meridional wind(m/s)	Temperature (K)	Specific humidity (g/kg)	Relative humidity (%)
1000	0.900	0.630	0.414	0.617	0.593	0.743
925	0.937	0.572	0.761	0.767	0.788	0.722
850	0.916	0.671	0.633	0.771	0.809	0.695
700	0.893	0.755	0.522	0.911	0.823	0.735
500	0.845	0.929	0.851	0.922	0.801	0.736
300	0.971	0.952	0.916	0.970	0.691	0.604
200	0.986	0.970	0.904	0.901	-	-

Table 1: Pre- monsoon 2013 Correlation Analysis of radiosonde data at Dhaka station and nearest grid point of JRA-55 reanalysis data at (a) 0000 UTC and (b) 1200 UTC

Table-2 Comparison Table

Parameters		DHK00Z SLCS days Mean	DHK00Z SLCS days Median	DHK00Z Sonde data	DHK00Z JRA-55 data	BB00Z JRA-55 data	BB06Z JRA-55 data	BB12Z JRA-55 data
Convective	KI (K)	27.6	29	**41.2**	**32.7**	**31.3**	**31.3**	**31.7**
	TT (K)	68	66.9	**70.2**	**72.5**	**74.2**	**70.5**	**81.5**
	SSI (K)	0.8	0.7	**-3.5**	**-0.4**	**-0.9**	1.7	1.1
	LI (K)	-0.2	0.1	**-3.8**	**-2.7**	**-3.17**	**-2.70**	**-0.84**
	PW (kg /m^2)	38.2	38.5	**49.5**	31.0	32.4	33.6	29.3
	CAPE (J/kg)	1363	1170	**1690**	**1409**	**1381**	**2207**	**1282**
	CIN (J/kg)	322	300	**278**	192	147	36	192
Kinematic	SHEAR0-500hPa (m/s)	16.7	16.5	**23.7**	**23.6**	**23.2**	**23.3**	**24.3**
	MS0-1km (m/s)	20	19.2	**27.7**	11.6	13.7	7.7	7.9
	MS0-2km (m/s)	16.7	16.2	13.9	9.8	10.4	7.2	5.7
	MS0-3 km(m/s)	15	14.6	11.3	8.2	8.7	6.2	5.2
	MS0-4 km(m/s)	14.3	13.9	8.5	7.6	7.7	6.4	5.7
	SREH (m^2 /s^2)	148	115	115	39	75	75	60
Combined	VGP0-1 km (m/ s^2)	0.59	0.58	1.20	0.41	0.51	0.36	0.28
	VGP0-2 km (m/s^2)	0.51	0.46	0.60	0.35	0.39	0.34	0.21
	VGP0-3 km (m/s^2)	0.46	0.42	0.49	0.29	0.32	0.29	0.19
	VGP0-4 km (m/s^2)	0.44	0.42	0.37	0.27	0.29	0.30	0.21
	EHI	1.32	0.43	**1.36**	0.31	0.65	1.05	0.49
	BRN	16.1	7.4	**20.53**	6.63	7.9	9.14	4.70

*DHK= Dhaka Station

**BB=Brahmanbaria (event location)

Table 2: Statistical mean (column 1) and median value (column 2) of convective parameters at 0000 UTC in Dhaka on SLCS days of Yamane et al. (2010b) are compared with Dhaka 0000 UTC sonde data (column 3) and Dhaka 0000 UTC with JRA-55 reanalysis data (column 4), Brahmanbaria at 0000 UTC, 0600 UTC and 1200 UTC JRA-55 reanalysis data on event day. The bold text represents that the value is in preferable side for storm genesis referencing to former studies.

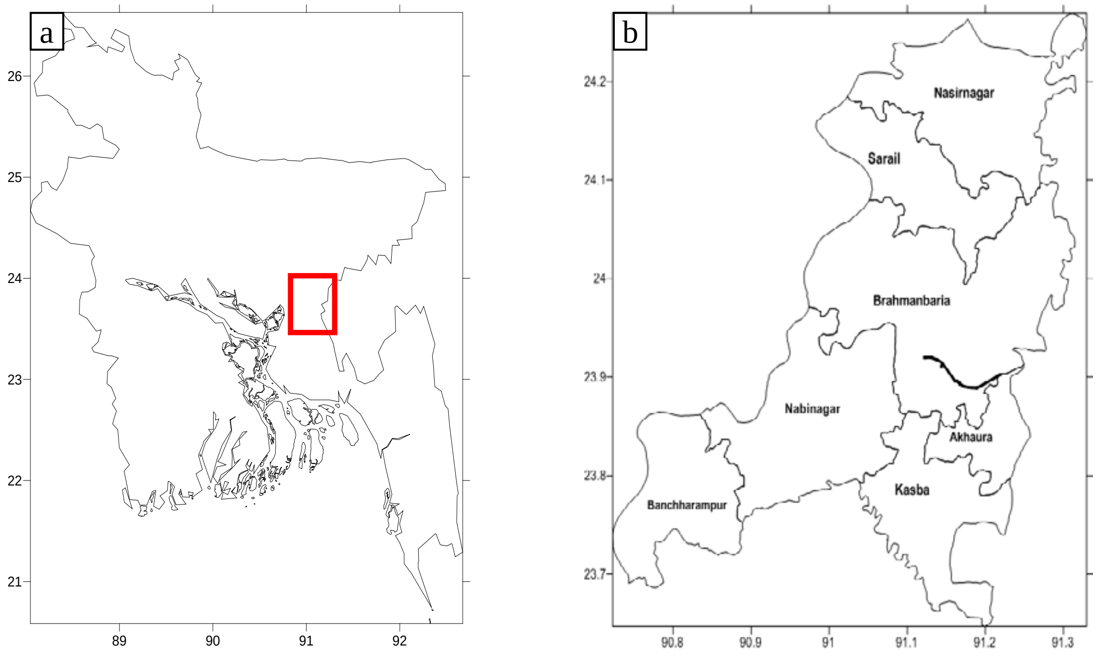

Fig 1: (a) Bangladesh territory and red box indicating Brahmanbaria district; (b) enlarged figure of red box indicating track of the tornado. GPS survey was conducted by the researchers of BMD and SMRC after the event occurrence.

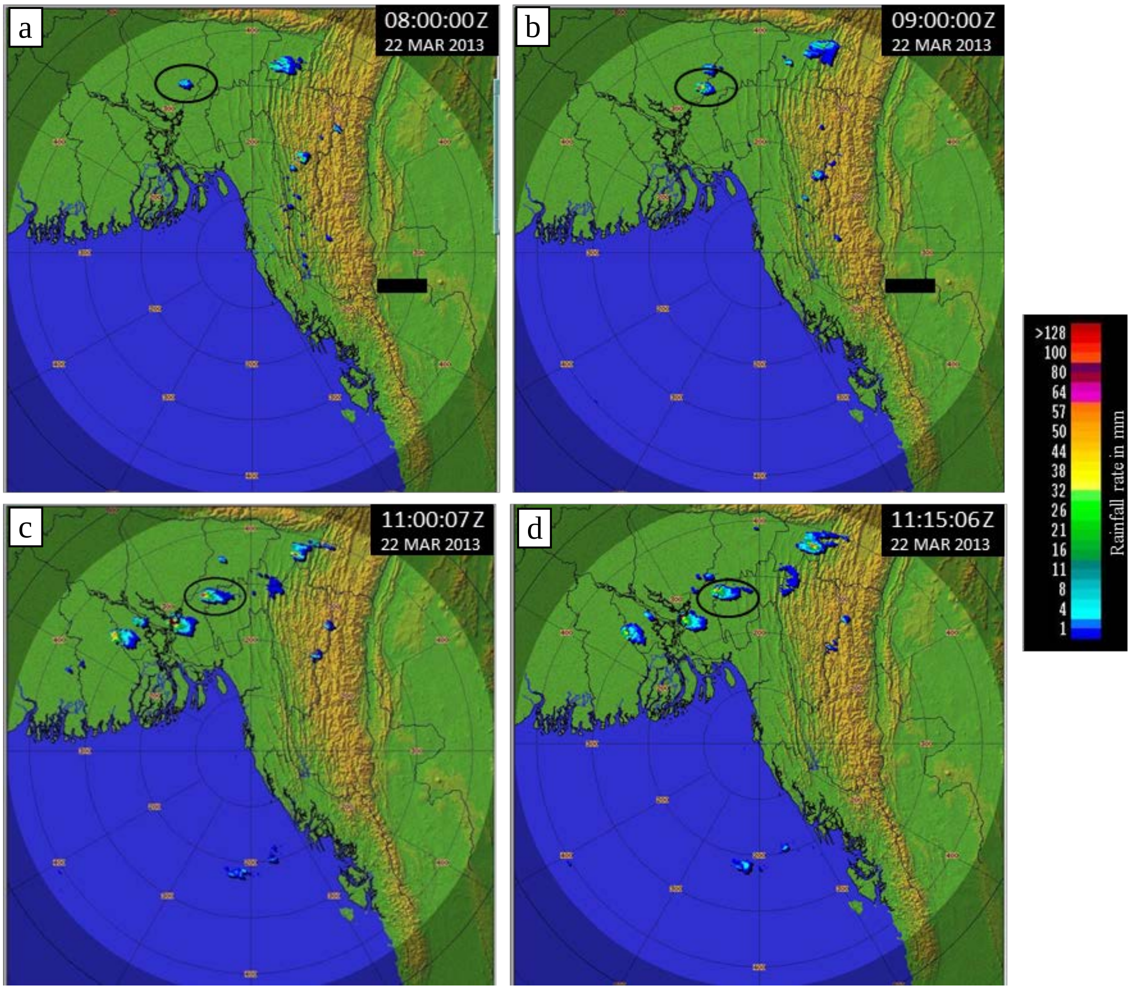

Fig 2: Cox’s Bazar radar images (a-d). The systems marked with thick black circle at a) 0800 UTC – system emerged, b) 0900 UTC - system intencified, c) 1100 UTC - event occurrence time and d) 1115 UTC -system moved south east ward. Rainfall intensity is presented in scale bar, the red color represents rainfall intensity of more than 100 (mm/hr). The center of the circle is the radar positon, and circles are drawn at every 100 km.

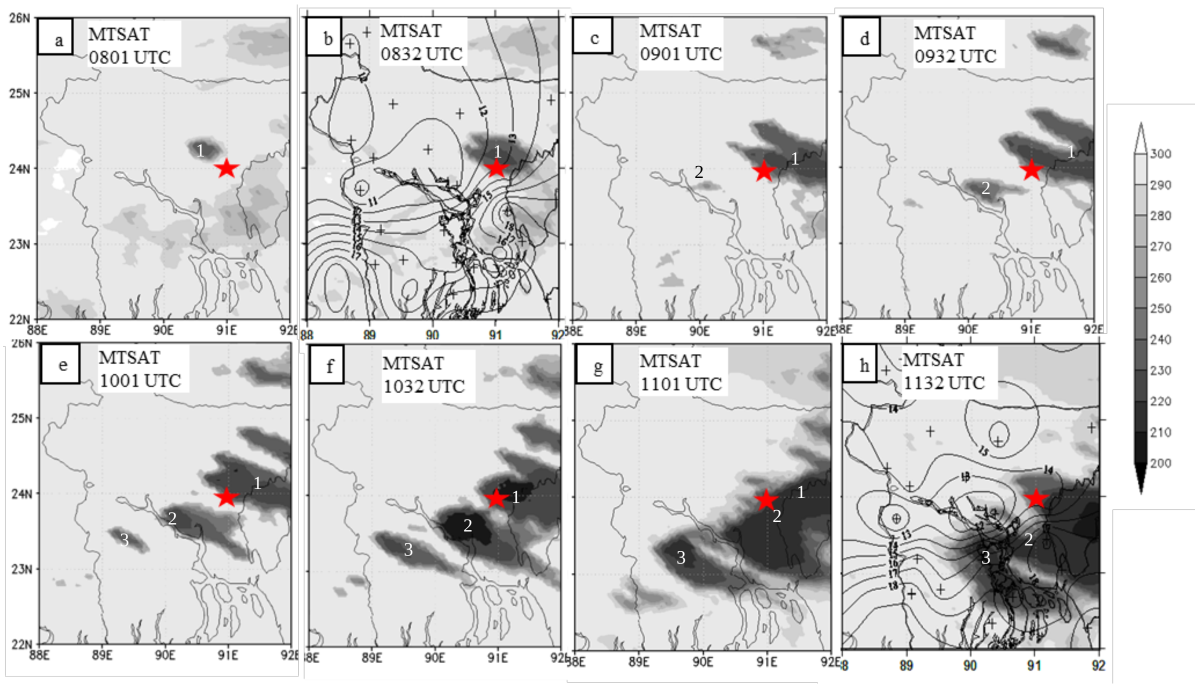

Fig 3: Shaded 30 min interval black body temperature (TBB) distribution by MTSAT-2 from 0801UTC to 1132UTC on 22 March 2013. Contoured surface specific humidity (g/kg) distribution of 0900 UTC and 1200 UTC of 3 hourly BMD SYNOP data overlaid with images (b) (h) respectively. Systems are recognized by no.1, 2 and 3. "Star" sign is event occurring region.

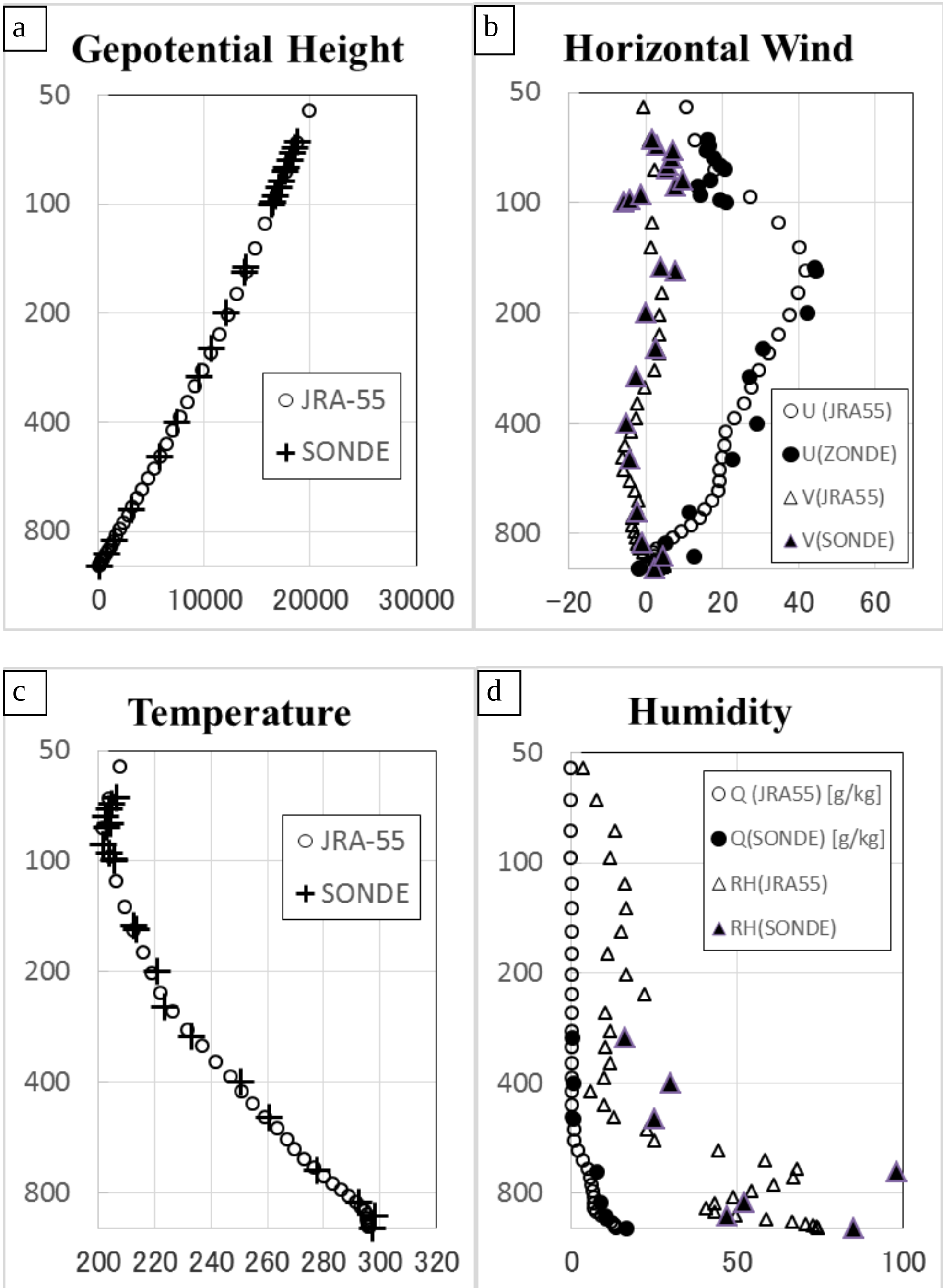

Fig. 4: Vertical profile of radiosonde data and JRA-55 reanalysis model level data of (a) Geopotential Heights, (c) Horizontal Wind (U and V component), (d) Temperature, (e) Relative Humidity (RH) and Specific Humidity (Q) at 0000 UTC 22 March, 2013

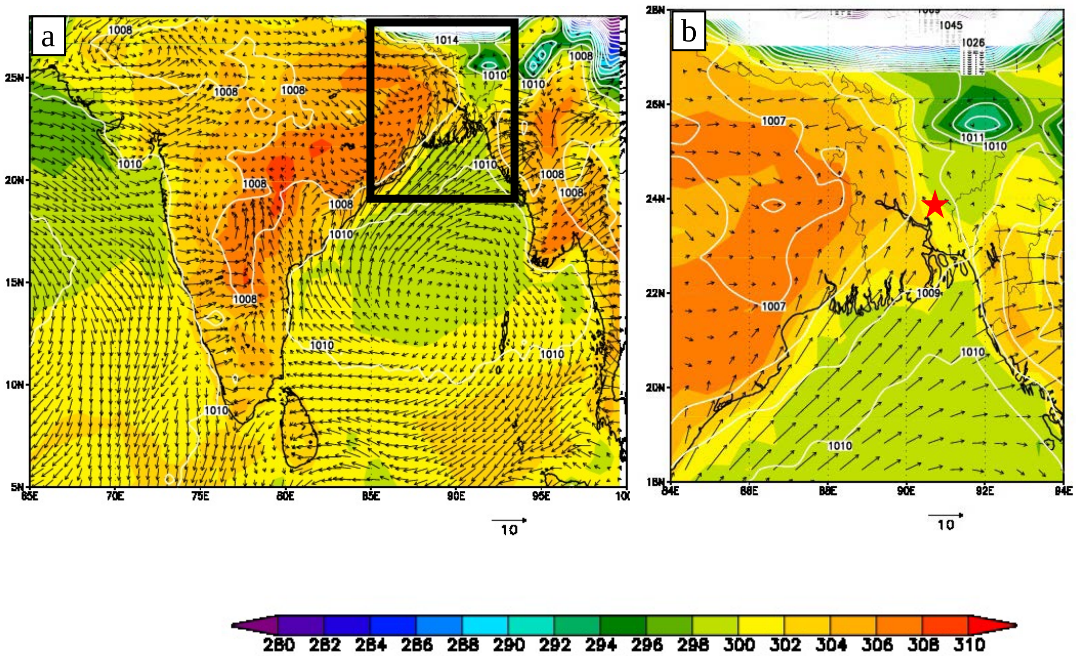

Fig. 5: Surface shaded temperature (K), vector wind (m/s) at lowest model level (approx.13m) and contoured MSLP (hPa) distribution at 0600 UTC over (a) Indian Subcontinent, black box indicating the smaller domain; (b) Bangladesh region (enlarged figure of red box) on 22 March 2013 by JRA-55 reanalysis data.

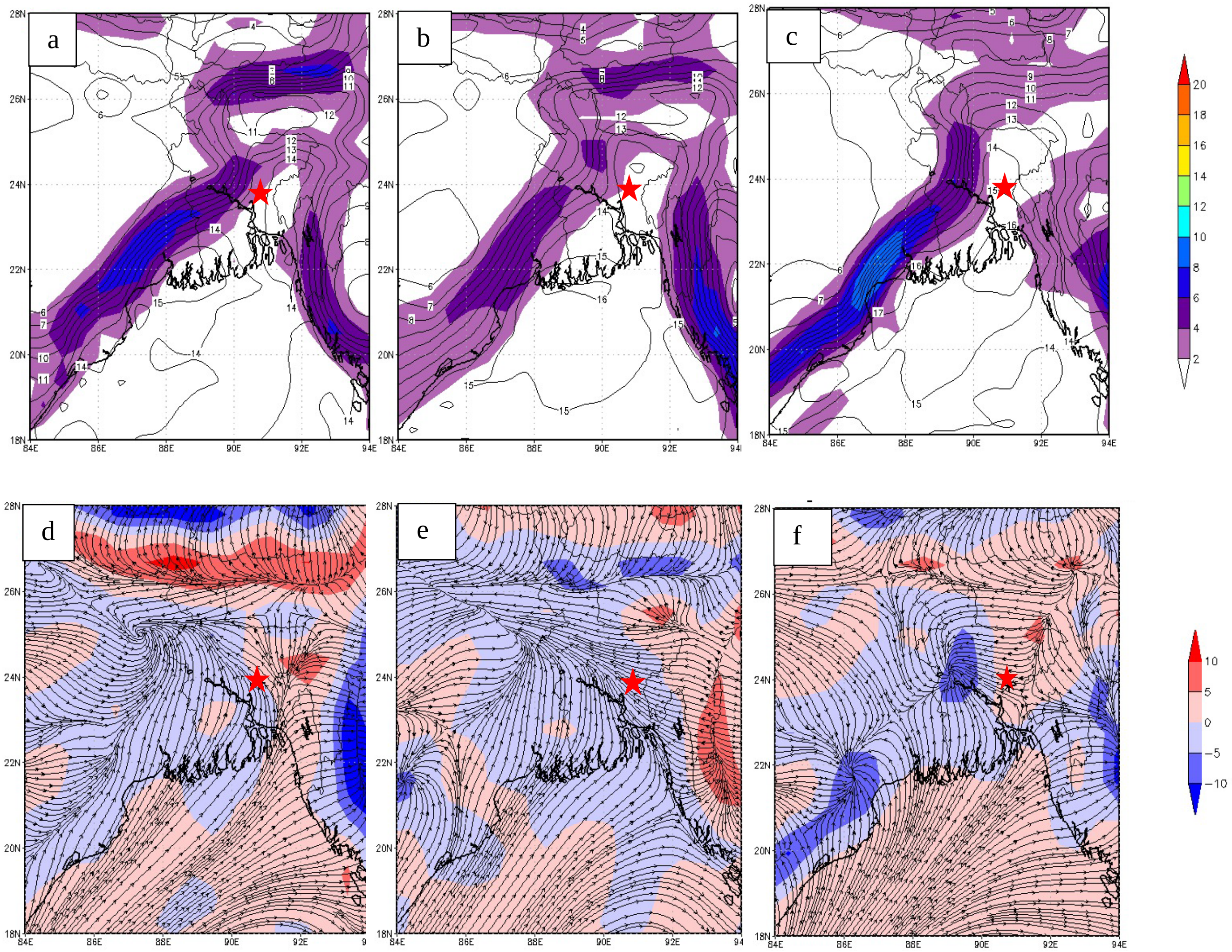

Fig. 6 Shaded surface specific humidity gradient (g/kg/100 km) and contoured surface specific humidity (g/kg) distribution at (a) 0000 UTC (b) 0600 UTC and (c) 1200 UTC; and Shaded surface divergence and streamline wind (m/s) at (d) 0000 UTC (e) 0600 UTC and (f) 1200 UTC over Bangladesh on 22 March 2013 by JRA-55 reanalysis data

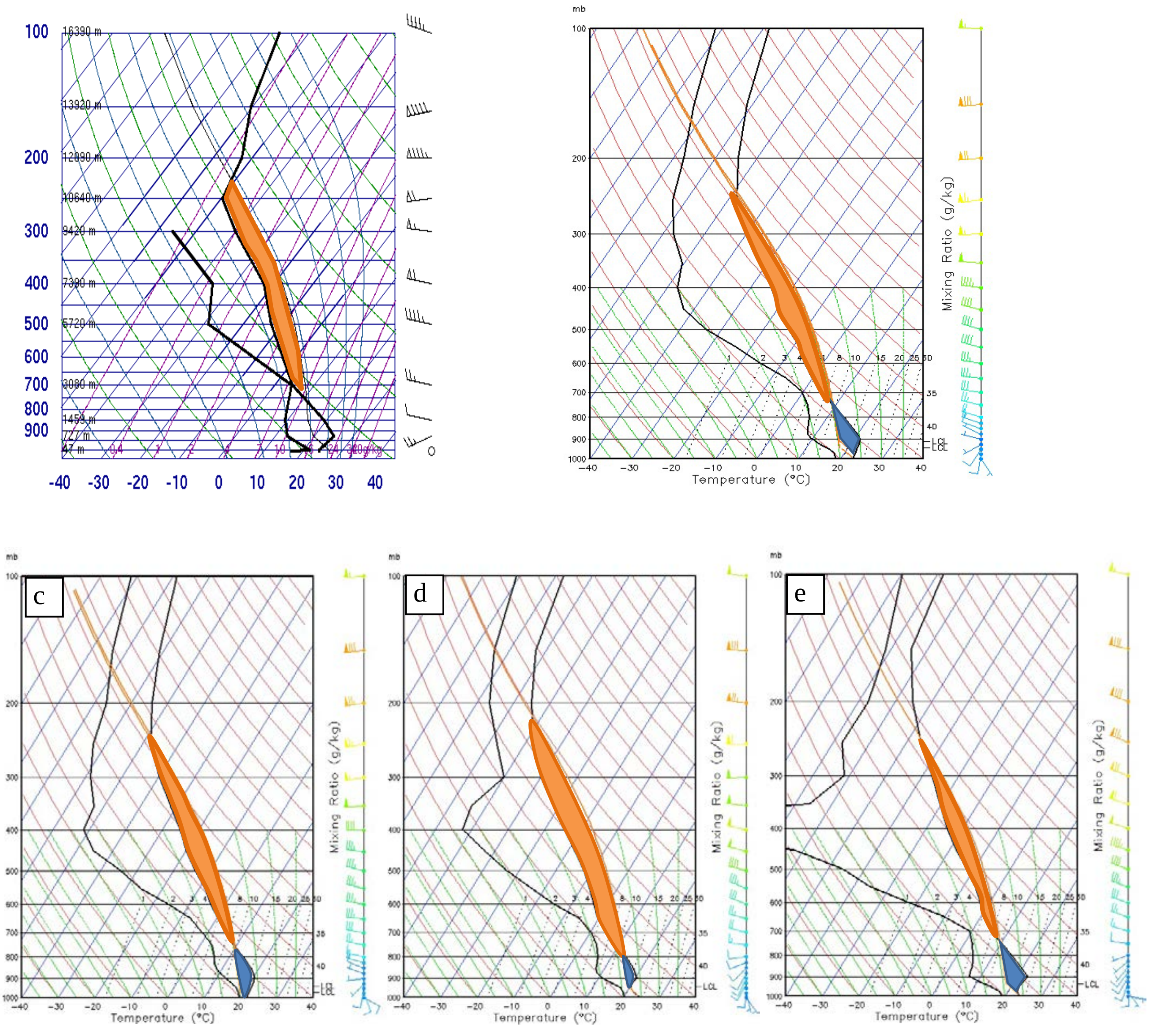

Fig. 7: Skew T/ log P analysis at 0000 UTC of a) Dhaka station radiosonde data from University of Wyoming archive, (b) JRA-55 reanalysis data at nearest grid of Dhaka Station; skew T/log P by JRA-55 reanalysis data of event location (24˚N latitude and 91˚E longitude) at (c) 0000 UTC, (d) 0600 UTC and (e) 1200 UTC on 22 March 2013

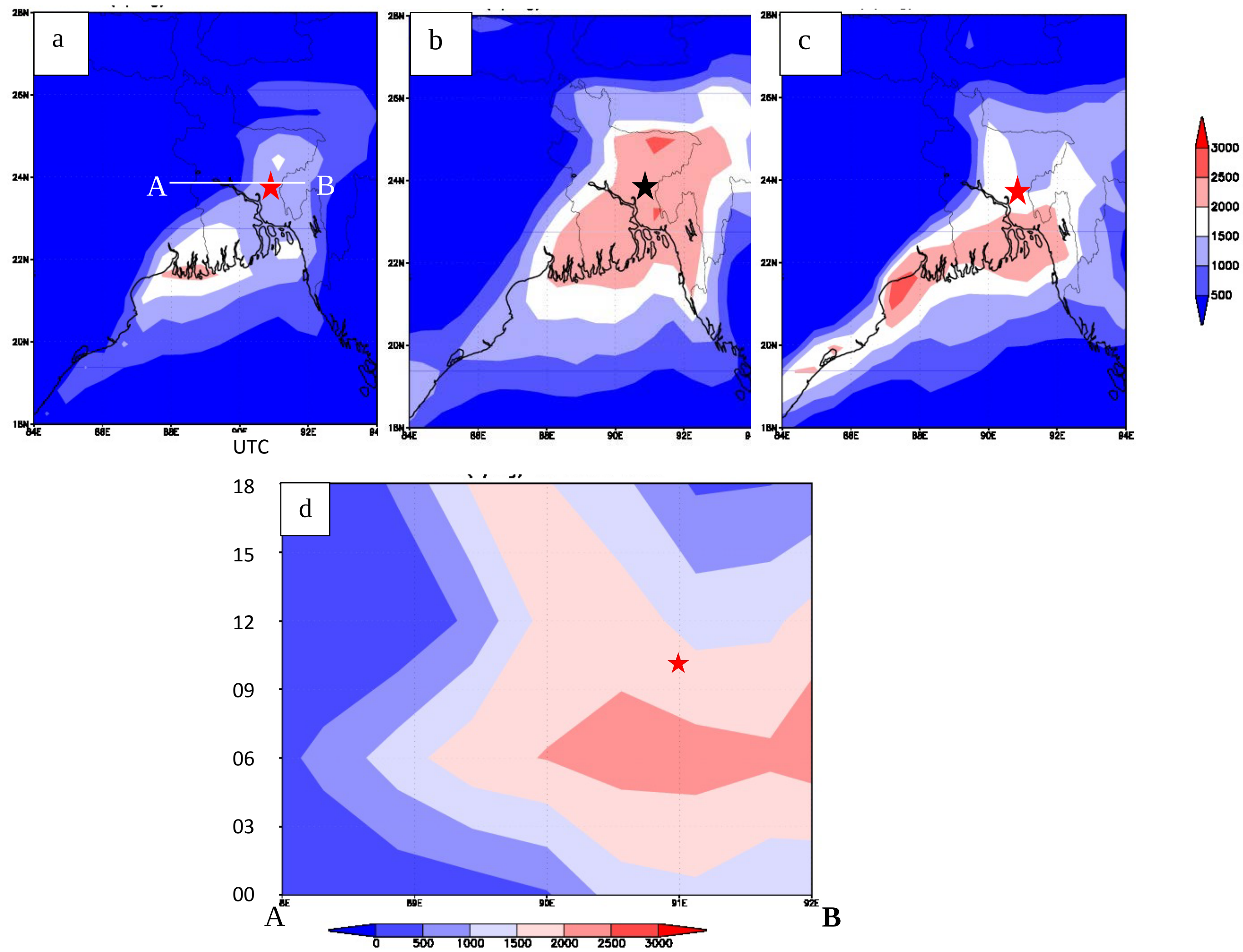

Fig. 8: Shaded CAPE (J/kg) distribution over Bangladesh at (a) 0000 UTC and (b) 0600 UTC (c) 1200 UTC and (d) time series at the cross section of 24˚N latitude (A-B line as 8a) from 0000 UTC - 1800 UTC on 22 March 2013 by JRA-55 reanalysis data

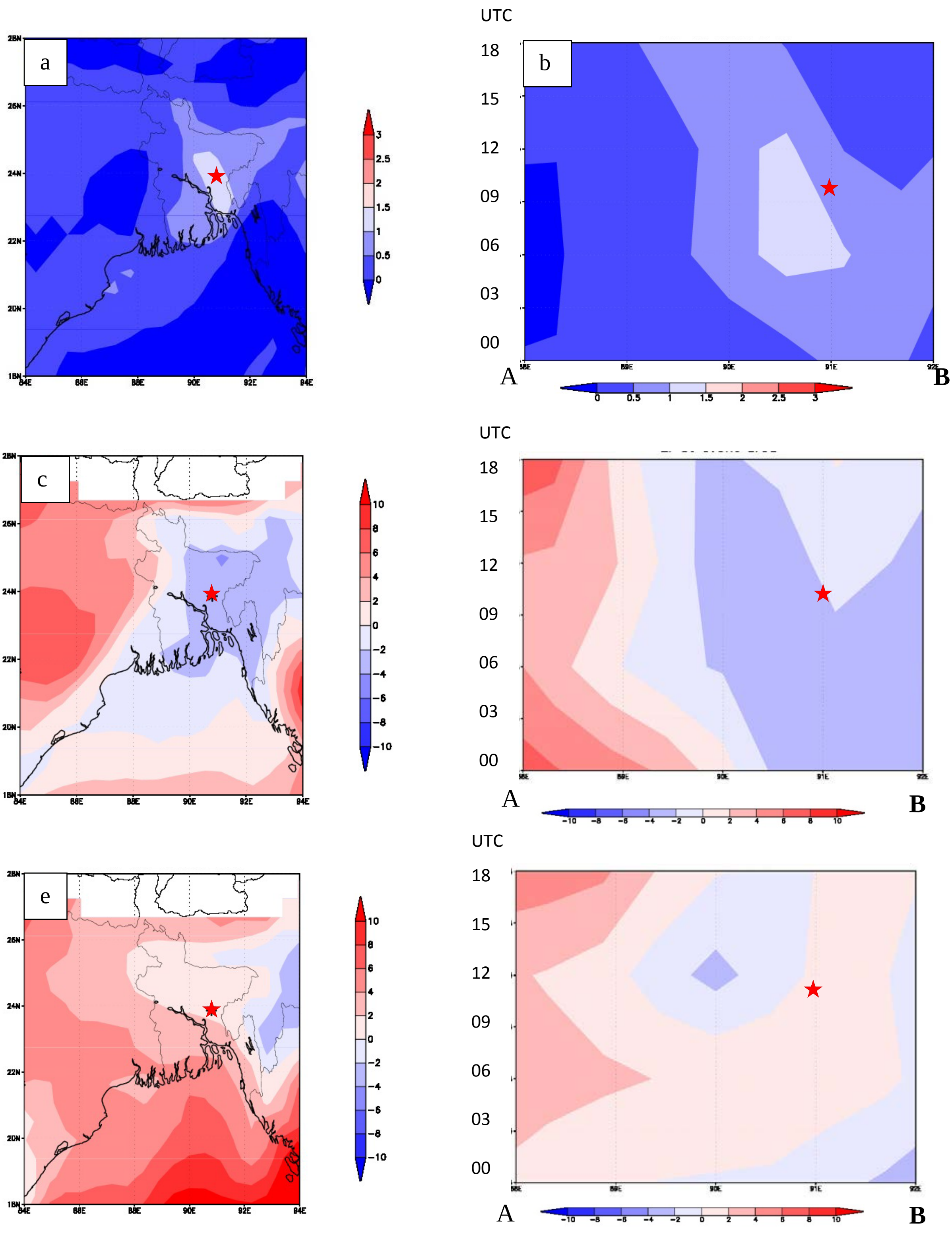

Fig.9: Spatial distribution of (a) EHI, (c) LI, and (e) SSI at 0600 UTC and time series at the cross section of 24˚N latitude (A-B line as 8a) from 0000 UTC - 1800 UTC on 22 March 2013 by JRA-55 reanalysis data